ACADEMIC PRESS

Available online at www.sciencedirect.com
SCIENCE DIRECT®

Journal of Catalysis 217 (2003) 1–11

JOURNAL OF CATALYSIS

www.elsevier.com/locate/jcat

Spectroscopic characterization of surface species in deactivation of sol–gel Gd–Pd catalysts in NO reduction with CH_4 in the presence of SO_2

Junko M. Watson and Umit S. Ozkan *

Department of Chemical Engineering, The Ohio State University, 140 W 19th Avenue, Columbus, OH 43210, USA

Received 20 June 2002; revised 20 November 2002; accepted 2 December 2002

Abstract

Titania-supported Pd catalysts prepared by the modified sol–gel method are effective NO reduction catalysts with CH_4 in the presence of oxygen and water. However, they were found to partially deactivate in the presence of SO_2. The effect of SO_2 on NO adsorption sites was investigated using in situ diffuse reflectance infrared Fourier transform spectroscopy and temperature-programmed desorption. The reversible NO adsorption capacity of the catalyst was significantly reduced following SO_2 exposure. SO_2 was also seen to inhibit the formation of linear Pd–NO species on the surface. It is suggested that partial loss of NO reduction activity could be related to the inhibition of the Pd–NO formation. Addition of Gd is found to partially prevent or slow down the deactivation process.
© 2003 Elsevier Science (USA). All rights reserved.

Keywords: Deactivation by SO_2; NO reduction with CH_4; DRIFTS; Gd–Pd catalyst; Sol–gel synthesis

1. Introduction

Nitric oxide reduction with hydrocarbons offers an attractive alternative to NH_3-SCR technology since the problems such as ammonia slip and transportation/storage that are associated with this technology can be eliminated. Using methane as a reducing agent especially has certain advantages since it is the least expensive lower hydrocarbon and exists abundantly in natural gas. Pioneering work on NO reduction with methane was studied by Li and Armor on metal exchanged zeolites [1–4]. Subsequently, numerous studies on the NO–CH_4–O_2 reaction have been performed on zeolitic systems [5–11]. NO reduction over rare earth oxides, such as La_2O_3, CeO_2, Nd_2O_3, Sm_2O_3, Tm_2O_3, and La_2O_3, has been found comparable to Co/ZSM-5 on a turnover frequency basis [12]. NO adsorption species on these systems and their thermal stability were characterized by in situ diffuse reflectance infrared Fourier transform spectroscopy (DRIFTS) [13]. Use of nanocrystalline Group IIIB metal oxides were shown to decrease the temperature required to activate methane [14].

In our earlier studies, we have investigated the use of CH_4 as a reducing agent for selective catalytic reduction of NO over Pd/TiO_2 catalysts in the presence of oxygen [15–18]. We have investigated the effect of oxygen concentration and temperature on the kinetics of the reaction [15]. The steady-state reaction experiments have shown that at certain critical oxygen concentrations at different temperature levels, regular and self-sustained oscillations were observed in both product and reactant profiles. These oscillations were concluded to be the result of cyclic phase transformations between Pd and PdO and were induced by the different levels of exothermicity of the reactions involved [17]. Temperature-programmed desorption (TPD) and isotopic labeling experiments combined with studies that used oscillations as a probe to understand the different catalytic pathways involved in NO–CH_4–O_2 reactions led us to suggest that NO reduction required the presence of Pd^0 sites where the formation of CH_x surface species took place. It was also suggested that CH_x species were involved in NO reduction, possibly forming a methyl–nitrosyl-type intermediate to give N_2. The experimental results also suggested that methane combustion, which is the favored reaction over the oxide phase, yields CO as a primary product, which under excess O_2 conditions, was further converted to CO_2. Our more recent studies have shown the effect of lanthanide elements in improving the oxygen resistance of the catalyst [24].

Since SO_2 and H_2O are always present in flue gas of stationary and mobile sources, further examination of their ef-

* Corresponding author.
E-mail address: ozkan.1@osu.edu (U.S. Ozkan).

0021-9517/03/$ – see front matter © 2003 Elsevier Science (USA). All rights reserved.
doi:10.1016/S0021-9517(02)00184-7

fects on the NO_x reduction reaction mechanism and catalyst activity is necessary. There have been several reports on the effect of SO_2 on NO reduction with lower hydrocarbons over different catalysts. Li and Armor investigated NO reduction by CH_4 in the presence of O_2 and SO_2 on Co-ZSM-5 and Co-ferrierite catalysts [19]. The effect of SO_2 on NO adsorption sites were investigated using temperature-programmed desorption. Over BSA (B_2O_3–SiO_2–Al_2O_3) supported platinum catalysts, it has been reported that 100 ppm of SO_2 improved the SCR activity using propene and depressed the formation of N_2O. The inhibition of N_2O formation was attributed to the retarded mobility of NO by SO_2 [20]. Li et al. investigated the NO reduction by ethylene in the presence of oxygen over Cu^{2+} ion-exchanged pillared clays. They reported that the effect of SO_2 was very mild and NO conversion decreased only slightly at 500 °C. However, at 350 °C, the deactivation was very severe possibly due to competitive adsorption on the active sites [21]. The effect of sulfur and sulfur compounds on the reduction of NO over noble metal automotive catalysts (Pt, Pd, Rd, and Ir on γ-Al_2O_3) under oxidizing and reducing conditions was examined by Gandhi and Shelef [22]. They found that the dispersion of metal particles on the support was an important factor on the oxidation of SO_2, and the activity of NO reduction to both dinitrogen and ammonia over the Pt and Pd catalysts was completely suppressed by the presence of very low levels of SO_2. They also concluded that, under oxidizing conditions, the sulfur storage capability of the support in the form of sulfate directly affected the poisoning resistance of the catalyst.

Previously, we have reported on the effect of H_2O and SO_2 on the activity of Pd catalysts supported over TiO_2 [23,24]. Addition of H_2O (7%) did not have any negative effect on the NO reduction activity of the catalyst, which maintained complete conversion over 18 h on stream. However, SO_2 was found to inhibit the NO conversion activity. When Gd was added to Pd/TiO_2, which was synthesized using a modified sol–gel method, it was shown to slow down the deactivation rate.

As a continuation of our earlier work, in this investigation, we examine the effect of SO_2 on NO adsorption sites using in situ diffuse reflectance infrared Fourier transform spectroscopy and temperature-programmed desorption.

2. Experimental

2.1. Catalyst preparation

Catalysts were synthesized using a modified sol–gel technique in which co-precipitation and sol–gel methods are incorporated as described elsewhere [24]. Catalyst synthesis included dissolving palladium acetate in isopropanol followed by addition of titanium isopropoxide. Gadolinium nitrate was added in aqueous form to the gellation medium during the hydration stage. The modified sol–gel method provides an intimate contact of the active catalyst components and the support material through the cogelling process. The metal loadings of the catalysts were 2% Pd/TiO_2 and 1% $Gd/2\%\ Pd/TiO_2$, by weight percentage.

The BET surface area measurement by N_2 adsorption resulted in the specific surface areas of 30, 51, and 62 m^2/g for TiO_2, 2% Pd/TiO_2, 1% $Gd/2\%\ Pd/TiO_2$, respectively.

2.2. Reaction studies

The steady-state reaction experiments were performed using a fixed-bed flow reactor (1/4-in od) made of stainless steel. The amount of catalyst packed was varied between 37.5 and 69 mg. The feed composition consisted of NO (500 ppm), CH_4 (1.06%), O_2 (2%), and SO_2 (145 ppm) in balance He at flow rates between 30 and 61 cm^3 (STP)/min. The reaction temperature was varied between 400 and 500 °C and was controlled by a PID temperature controller (Omega). In each reaction, the sample was prereduced using a mixture of 33% H_2 in He at 200 °C for 30 min. The feed and effluent streams were analyzed online using a combination of a gas chromatograph (5890A HP), a chemiluminescence NO–NO_2–NO_x analyzer (Themo Environmental Instruments, Model 42H), an IR ammonia analyzer (Siemens Ultramat 5F), and pulse fluorescence SO_2 analyzer (Thermo Environmental Instruments, Model 43C). The gas chromatograph was equipped with a 10 ft × 1/8-in Porapaq Q column and a 8 ft × 1/8-in molecular sieve column to quantify N_2, O_2, CO, CO_2, CH_4, N_2O, and SO_2. In all experiments, nitrogen and carbon balances closed within 5%.

2.3. Catalyst characterization

Temperature-programmed desorption experiments were performed using a TPR/TPD flow system equipped with a thermal conductivity detector described elsewhere [15]. The desorption species were monitored by a HP5890GC-MS. The sample (75 mg) was loaded to the U-shaped quartz reactor and calcined in situ in 10% oxygen in balance helium at 500 °C for 0.5 h followed by flushing in helium for 30 min. Next, the samples were reduced in 33% hydrogen in balance helium at 200 °C for 30 min followed by flushing for 30 min in helium. SO_2 pretreatment was performed after the reduction step using 1% SO_2 in He for 2 h at 500 °C followed by He flushing for 1 h at 500 °C. Subsequently, the catalyst was cooled to room temperature under helium flow. Adsorption of gas was performed at room temperature for 1 h followed by helium flushing for 1 h to remove physically adsorbed gas.

Diffuse reflectance infrared Fourier transform spectroscopy experiments were performed using a Bruker IFS66 equipped with a DTGS detector and a KBr beamsplitter. Catalysts were placed in a sample cup inside a Spectratech diffuse reflectance cell equipped with KBr windows and a thermocouple mount that allowed direct measurement of the surface temperature. Each catalyst was pretreated in situ either by calcination under 10% oxygen at 400 °C

surface temperature or by reduction under 30% hydrogen in balance helium at 200 °C surface temperature for 30 min. Sulfation of the samples was carried out at 300 °C with 1000 ppm SO_2 in He for 30 min. Background spectra were recorded after pretreatment at each temperature level. For sequential adsorption at 300 °C surface temperature, background spectra were taken at 300 °C under helium before adsorption gases were introduced. For adsorption spectra obtained at several different temperature levels, background spectra were taken at each temperature level under helium prior to the introduction of the adsorption gas. Each spectrum was averaged over 1000 scans in the mid-IR range (400–4000 cm^{-1}) to a nominal 2 cm^{-1} resolution.

3. Results and discussion

3.1. Effect of SO_2

To design a NO_x reduction catalyst which is highly resistant to SO_2, it is important to study the deactivation mechanisms. The effect of SO_2 was investigated under steady-state reaction conditions over two different catalysts, namely 2% Pd/TiO_2 and 1% $Gd/2\%\ Pd/TiO_2$. These results were presented previously [24]. Although both catalysts lost some activity when exposed to SO_2 over extended periods of time, addition of Gd was found to be quite effective in slowing down the deactivation of the Pd-containing catalysts. Gd–Pd catalysts showed a significant decrease in SO_2 deactivation rate compared to the Gd-free catalysts. After 5 h online, the NO conversion level was at 70%, which was more than a two-fold increase compared to that of Pd/TiO_2. The conversion level seemed to reach a plateau at the end of 20 h at around 45%.

3.2. Effect of SO_2 on surface species during $NO + CH_4 + O_2$ reaction

In situ DRIFTS was used to investigate the effect of SO_2 on surface species during the reaction of $NO + CH_4 + O_2$. Previously, we reported an extensive investigation of the adsorbed species under steady-state and transient conditions on sol–gel prepared Pd catalysts using this technique [25,26]. It was found that linearly adsorbed NO on Pd, which has a vibrational frequency at 1789 cm^{-1}, was the predominant species under $NO + CH_4 + O_2$ flow at 300 °C on Pd catalysts supported on TiO_2 [25,26]. The effect of a low concentration of SO_2 on adsorbed species under $NO + CH_4 + O_2$ flow at 300 °C was examined by sending pulses of SO_2 to the reaction mixture. The $Gd–Pd/TiO_2$ catalyst was reduced in 33% H_2/He mixture at 200 °C for 30 min followed by He flushing. The background spectrum was taken in He at 300 °C after the reduction step. The catalyst was then exposed to a reaction mixture of NO, CH_4, and O_2 at 300 °C. After the reaction reached steady-state, pulses (1 cm^3) containing 37 ppm SO_2 were introduced to the reaction mixture using a six-way port valve. Fig. 1 shows the spectra taken after SO_2 pulses on Pd/TiO_2. The first spectrum was taken under SO_2-free flow. The next seven spectra were taken after each successive SO_2 pulse, 1 through 7. The spectrum at the top was taken after the 27th pulse. Before SO_2 introduction, bands were observed at 1789, 1609, 1536, 1439, 1356, and 1301 cm^{-1}. The band at 1789 cm^{-1} has been identified as linearly adsorbed NO on Pd in the literature [27–30]. This peak was seen to shift toward higher wavenumbers after each SO_2 pulse. After 27 pulses, the linear NO peak that originally appeared at 1789 cm^{-1} shifted to 1811 cm^{-1} indicating that the bond between NO and Pd was weakened by the presence of sulfur containing species, getting closer to gas phase NO, which has a vibrational frequency of 1875 cm^{-1}.

The band at 1609 cm^{-1} in Fig. 1 was attributed to bridged nitrate [31–34]. The band at 1301 cm^{-1} is due to gas phase methane. Monodentate nitrate species have vibrational frequencies at 1530–1480 cm^{-1} ($NO_{2,asy}$) and 1330–1250 cm^{-1} ($NO_{2,sym}$) [31–33]. The frequency of the NO_{2sy} band and the rotational frequencies present above and below 1301 cm^{-1} for methane overlap make it difficult to identify the $NO_{2,sym}$ band. The broad feature at 1536 cm^{-1} could be assigned to monodentate nitrate species. In addition, the broad features of 1536 and 1439 cm^{-1} have been attributed to nitro–nitrito complex in the literature [44]. It is possible that both monodentate nitrate and nitro–nitrito complex are present on the surface. These bands did not seem to be affected by the presence of SO_2.

There was a pair of bands at 1356 and 1168 cm^{-1} growing in intensity after each SO_2 pulse. Weakly adsorbed SO_2 has been reported to have vibrational frequencies around 1335–1360 cm^{-1} in the literature [35,36]. A rapid growth of the band at 1356 cm^{-1} was attributed to S=O stretching mode [37]. Datta and Cavell studied SO_2 adsorption on alumina catalysts and observed bands at 1050, 1134, and 1322 cm^{-1}. In the hydroxyl region, they observed a disappearance of the 3680 cm^{-1} band accompanied by a broad band around 3550 cm^{-1}, indicating the interaction of SO_2 molecules directly with the 3680 cm^{-1} hydroxyls [45]. In our case, we also observed a growing negative peak at 3669 cm^{-1} accompanied by a broad band at 3583 cm^{-1} (Fig. 1). The surface species that are associated with the bands mentioned above have been identified as sulfite-like species on basic sites (negatively charged oxygen ions) [26].

The spectra taken over the $Gd–Pd/TiO_2$ catalyst under the same experimental conditions are shown in Fig. 2. Before SO_2 introduction, the major difference between the two catalysts is that, in the presence of Gd, linear NO species (1792 cm^{-1}) on Pd is much more prominent relative to the nitrate species. Over the Gd/Pd catalyst, similar to what was observed over the Pd-only catalyst, the band position of linear Pd–NO was seen to gradually shift to higher frequencies with each SO_2 pulse. However, the shift was much smaller over the Gd/Pd catalyst, changing the band position from 1792 to 1805 cm^{-1} by the 27th pulse. Even

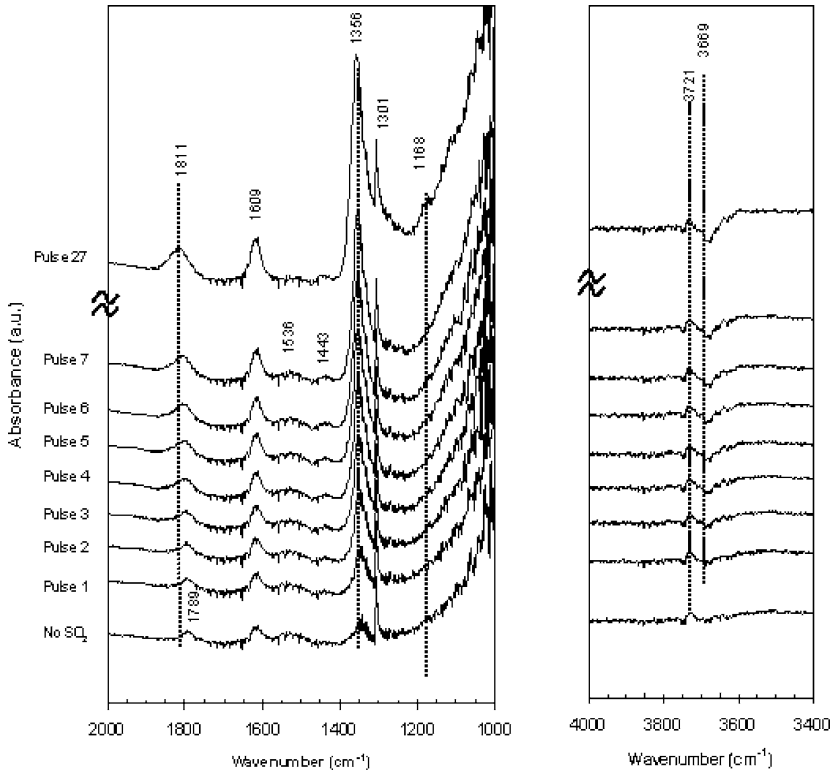

Fig. 1. In situ DRIFT spectra of Pd/TiO_2 after pulses of 37 ppm SO_2 were introduced to the feed containing 1780 ppm NO, 2.13% CH_4, 3000 ppm O_2 in He at 300 °C.

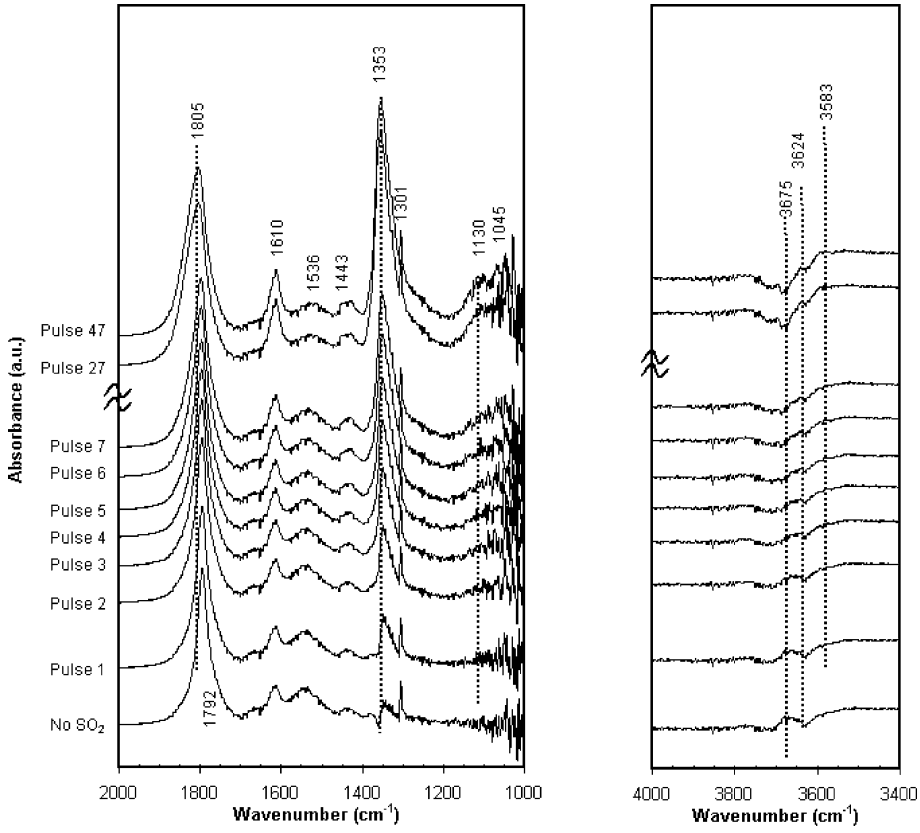

Fig. 2. In situ DRIFT spectra of $Gd–Pd/TiO_2$ after pulses of 37 ppm SO_2 were introduced to the feed containing 1780 ppm NO, 2.13% CH_4, 3000 ppm O_2 in He at 300 °C.

after the 47 pulses, the shift was still smaller than what was seen over the Pd-only catalyst after 27 pulses (13 vs 22 cm^{-1}).

Similar shifts in this band were observed in SO_2-free environments where the increase in temperature and/or the presence of oxygen in the flow mixture was seen to cause a shift toward higher frequencies [26]. A series of IR experiments suggested that the position of the band which appeared around 1772–1792 cm^{-1} was affected by the state of Pd, which was directly influenced by surface oxygen concentration [45]. As the surface becomes more oxidized, electronegativity of oxygen reduces the electron density at Pd atom, which consequently weakens the backbonding to antibonding orbital of NO, causing the Pd–NO band location to shift toward higher wavenumbers. It appears that the presence of SO_2 is having a similar effect and weakening the Pd–NO bond, as indicated by the band shift. This could be due to the formation of sulfite-like species on the surface. It could signal a change in the oxygen density surrounding the Pd atom, bringing it closer to a higher oxidation state.

Our previous results through controlled-atmosphere XPS have shown that the Pd and Gd–Pd catalysts lose activity when palladium is completely oxidized to PdO [24]. The smaller shift in Pd–NO band for the Gd–Pd catalyst is consistent with the reaction data, which showed a slower deactivation rate over the Gd/Pd catalyst. It is also consistent with the earlier conclusion that Gd can inhibit the oxidation rate of Pd compared to the Gd-free catalyst. The stabilizing role of Gd in maintaining the Pd in metallic state appears to be in effect whether the oxidizing environment is created by the presence of SO_2 or O_2, which manifests itself in the form of a higher resistance to SO_2 deactivation.

Previously, we studied NO reduction with CH_4 with different oxygen concentrations on Pd/TiO_2 and lanthanide element-doped Pd/TiO_2, such as Ce–Pd, Yb–Pd, and Gd–Pd supported on TiO_2 [24]. On the lanthanide-free catalyst, the catalyst lost NO reduction activity at a lower oxygen concentration (much lower than stoichiometric) compared to the lanthanide-doped catalysts where it remained active under excess oxygen conditions. Pd 3d X-ray photoelectron spectra of Pd/TiO_2 and $Gd–Pd/TiO_2$ after the catalysts were exposed to a reaction mixture with near stoichiometric O_2 concentration showed that Pd was completely converted to PdO on Pd/TiO_2 (deactivated) while the majority of Pd in $Gd–Pd/TiO_2$ was stabilized in the zero oxidation state (active). Similar results were obtained with a lanthanide–palladium nanoscale bimetallic catalytic system which was synthesized using $\{(DMF)_{10}Ln_2[Pd(CN)_4]_3\}$ (Ln = Yb, Sm) as precursors for the $NO–CH_4–O_2$ reaction [46]. TEM micrographs showed that Yb or Sm metal and Pd metal were in intimate contact at the atomic level. This intimate contact of the lanthanide element and Pd was suggested as the reason Pd remained in the metallic phase under more oxidizing conditions than Pd alone [46]. The electropositive nature of lanthanide metal could possibly inhibit the oxidation of the precious metal. Higher SO_2 resistance in the presence of Gd could also be attributed to the electropositivity of Gd, which helps Pd to remain in the zero oxidation state in the presence of SO_2. In addition, more active sites could be created due to the presence of Gd, which simply provide adsorption sites for SO_2 thereby preventing adsorption on Pd sites.

3.3. Temperature-programmed desorption

The effect of SO_2 on NO adsorption sites and desorption behavior was studied by comparing the NO TPD profiles obtained over reduced and sulfated catalysts. Pd/TiO_2 and $Gd–Pd/TiO_2$ catalysts were sulfated under 1% SO_2 at 500 °C for 1 h followed by He flushing. The sample was then cooled for NO adsorption at room temperature. Temperature-programmed desorption profiles for NO from freshly reduced and sulfated samples are compared in Figs. 3 and 4.

Fig. 3 compares NO TPD profiles of reduced and sulfated Pd/TiO_2. The desorption features on the reduced catalyst were observed at 108, 173, and 256 °C (shoulder). After sulfation of the catalyst, the peak intensity was suppressed and the line shape was broadened. The high temperature feature at 256 °C disappeared completely over the sulfated catalyst.

Over the reduced Gd–Pd catalyst in Fig. 4, the NO desorption temperatures observed were the same as the reduced Pd catalyst. However, the relative intensity was strongest at the highest temperature (256 °C). On the sulfated catalyst, the low- and mid-temperature features were still present;

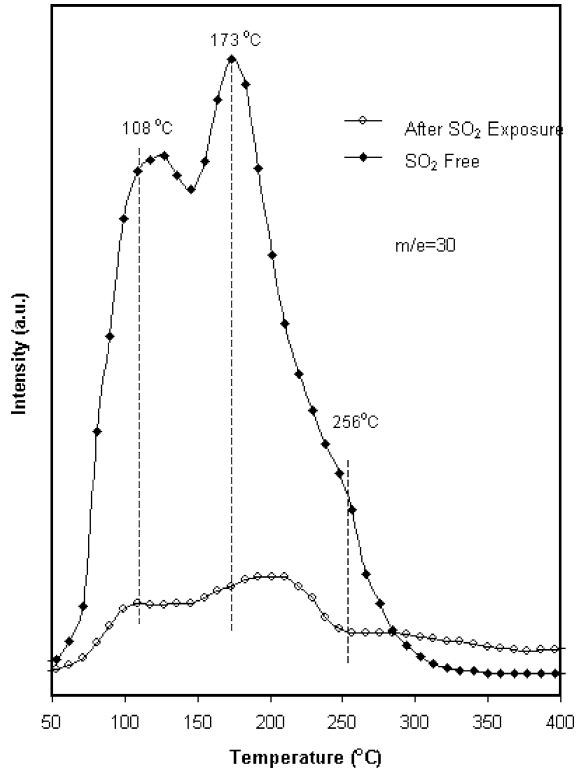

Fig. 3. NO TPD profiles for reduced Pd/TiO_2 and sulfated Pd/TiO_2.

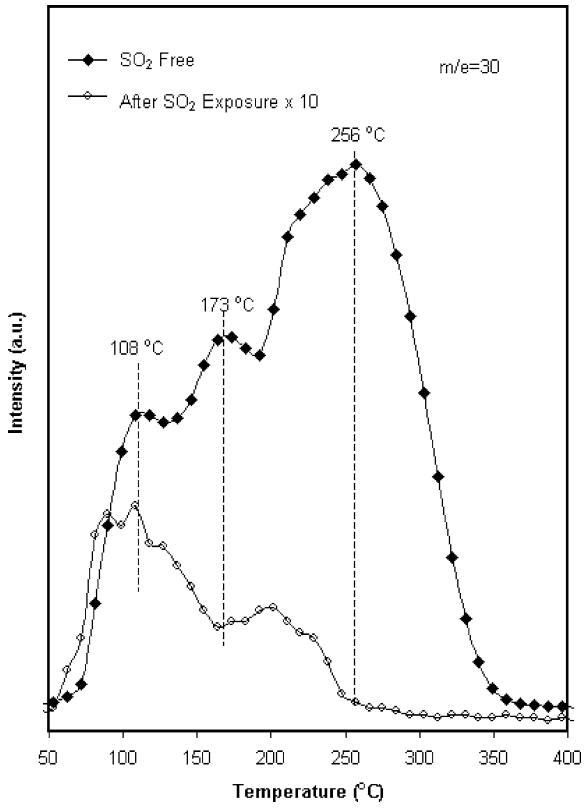

Fig. 4. NO TPD profiles for reduced Gd–Pd/TiO_2 and sulfated Gd–Pd/TiO_2.

however, the peak at 256 °C disappeared completely, similar to what was observed in Fig. 3. Furthermore, the total amount of reversibly adsorbed NO was significantly reduced when the catalyst was sulfated.

To summarize the TPD results on sulfated catalysts, the high temperature feature of both catalysts was greatly affected by sulfation. The absence of this feature on sulfated catalysts implies that Pd–NO species were not formed as readily, possibly due to site blockage. On TiO_2-supported catalysts, the total NO adsorption capacity was substantially decreased. On Co-ZSM-5 catalyst, Li and Armor showed a similar result where a complete disappearance of NO desorption peak at the highest temperature was noted when the catalyst was sulfated, where they also observed a total of 30% reduction in available NO adsorption sites [19].

3.4. DRIFT spectra of adsorbed SO_2 species

Over the reduced TiO_2 and Gd–Pd/TiO_2, a flow of 1000 ppm SO_2 in He was introduced at 300 °C and spectra were taken after 1, 11, 21, and 31 min of SO_2/He flow (Figs. 5 and 6). Here DRIFT spectra of SO_2 adsorption on Pd/TiO_2 are omitted as the types of adspecies observed on Pd/TiO_2 are the same as those formed on Gd–Pd/TiO_2. The surface was then flushed with He at the same temperature after which another spectrum was taken. Under SO_2 flow, several bands at 1420, 1371, 1331, 1203, and 1037 cm^{-1} were observed on TiO_2 (Fig. 5). The band at 1420 cm^{-1} has been observed by Yang et al. on sulfated sol–gel TiO_2 and Degussa TiO_2, but the band assignment was not given [35]. The bands at 1371 and 1203 cm^{-1} were observed immediately after the SO_2 flow was started, but decreased in intensity under He flow, which indicated that they are likely to be weakly adsorbed SO_2 species. The bands in the 1300–1400 and 1100–1200 cm^{-1} regions are assigned to the asymmetric and symmetric stretching vibrations of SO_2, respectively. The band observed at around 1331 cm^{-1} can be attributed either to a scissor-like bending mode of adsorbed H_2S [37,47] or sulfite-like species [40]. But SH_2 bands should be accompanied by another band at 2560 cm^{-1}, which is attributed to S–H stretching. This band was absent in our spectrum, suggesting that formation of H_2S could be excluded. The band at 1203 cm^{-1} has been reported to be sensitive to evacuation on $MgAl_2O_4$ below 200 °C [40]. This band could be due to S=O stretching in a sulfite-type species.

Wang and Li [40] studied the thermal stability of adsorbed SO_2 species on magnesium-aluminate spinel sulfur transfer catalyst. Using FTIR spectroscopy, they observed bands at 1330, 1150, and 1040 cm^{-1} developing under SO_2 flow, which were attributed to sulfite-like species. They also observed that the species which gave rise to the 1150 cm^{-1} band were weakly adsorbed as they desorbed very easily under vacuum. In the hydroxyl region, we observed a growing negative peak at 3678 cm^{-1} accompanied by a broad band at 3557 cm^{-1}, suggesting interaction of SO_2 with the surface OH groups.

On Gd–Pd/TiO_2 catalyst, the bands formed due to SO_2 adsorption are similar to those on the support (1424, 1344, 1203, 1153, and 1040 cm^{-1}) (Figs. 5 and 6). However, the relative intensities of these bands were different between the two samples. When Figs. 5 and 6 are compared, the peak intensity of band $\sim$1340 cm^{-1} was noticeably increased on the Gd–Pd catalyst compared to the support material after the same sulfation treatment. This is likely due to adsorption of SO_2 on Pd sites. The band at 1203 cm^{-1} also is much more intense over the catalyst than it is over the bare support. If this band were indeed due to a sulfite-like species, one would expect the formation of these species to be enhanced over the catalyst surface as compared to the bare support. The presence of Pd is likely to increase the oxygen mobility of the support, and hence enhancing the transformation of SO_2 on the surface to sulfites species. An equally likely possibility is the dissociative adsorption of SO_2 on the Pd surface, leaving adsorbed oxygen species behind, which are subsequently used for conversion of SO_2 to SO_3.

3.5. DRIFT spectra of adsorbed NO species on sulfated surface

NO (5000 ppm in He) was adsorbed on sulfated TiO_2 and Gd–Pd/TiO_2 samples at room temperature. The sulfation was conducted at 300 °C with 1000 ppm SO_2 for 30 min over

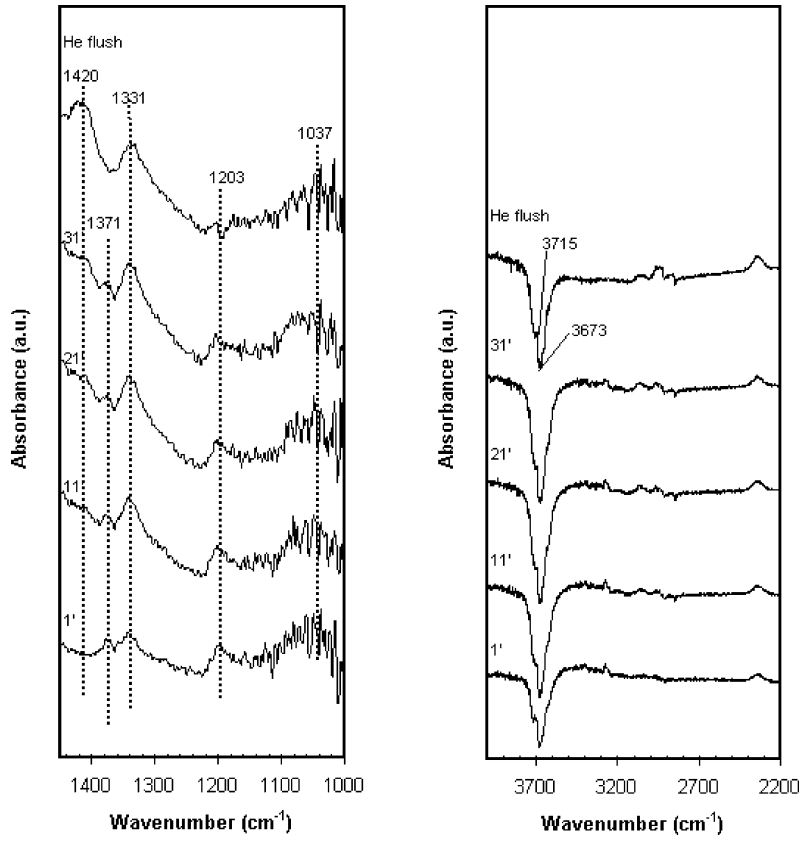

Fig. 5. DRIFT spectra of TiO_2 under 1000 ppm SO_2 in He flow.

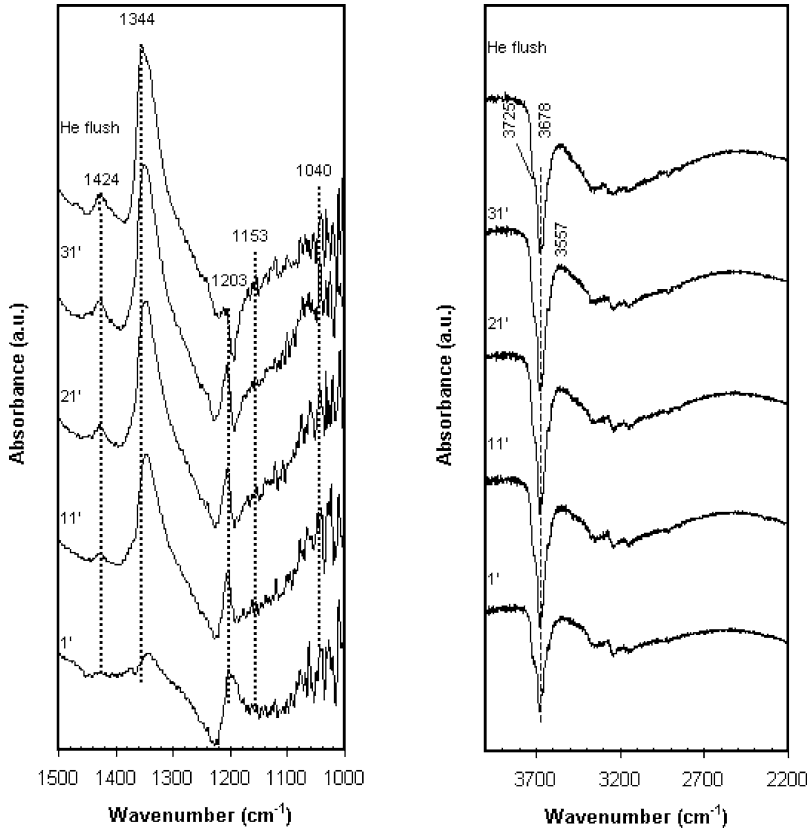

Fig. 6. DRIFT spectra of Gd–Pd/TiO_2 under 1000 ppm SO_2 in He flow.

prereduced samples. The background spectrum was taken at room temperature under He after sulfation of the catalysts. The spectra taken under NO flow at 1, 7, 12, and 21 min are presented in Figs. 9 and 10 for TiO_2 and Gd–Pd/TiO_2, respectively.

Several bands appeared immediately after NO introduction. The band at 1874 cm^{-1} corresponds to gas phase NO. There were strong bands at 1688/1244/3536 cm^{-1} on both TiO_2 and Gd–Pd/TiO_2 that grew in intensity over time suggesting that these species are most likely formed on the titania surface. The 3536 cm^{-1} band is a characteristic frequency of OH, the 1688 cm^{-1} band is an asymmetric deformation of NO_2, and the 1244 cm^{-1} band is for symmetric stretching vibration in NO_2 [49]. These bands could result from HNO_2-like species. The negative band in the 3600–3700 cm^{-1} region could be due to the disappearance of OH vibrations in surface complexes such as SO_2–OH, which could have formed during the SO_2 treatment.

There are bands that grow with time under NO flow at 1519/1272 cm^{-1} and 1603 cm^{-1} that were assigned to monodentate nitrate and bridging nitrate, respectively [31–33]. These bands were also observed on unsulfated TiO_2 [25,26]. The bands around 1360 and 1420 cm^{-1} have been assigned to nitro species [44]. The 1754 cm^{-1} band, which only appeared on Gd–Pd/TiO_2 in weak intensity, could be assigned to linear NO adsorbed on metallic Pd sites (Pd^0–NO). The band position is lower than that observed when NO is adsorbed on S-free Pd surfaces. This could possibly be explained by the dipole coupling effect, which at higher surface coverages, causes a blue shift in the Pd–NO band position. If SO_2-treatment causes Pd sites to be partially covered, this would decrease the number of Pd sites available for NO adsorption, hence resulting in a much lower surface coverage for NO species. This, in turn, would reduce the dipole coupling effect, shifting the band position back to lower frequencies. A second possibility for the assignment of the 1754 cm^{-1} band is that it could be due to N_2O_4 species. In the literature, the feature at 1755–1751 cm^{-1} has been also assigned to N_2O_4, and considering that the SO_2 treatment is likely to increase the oxidized Pd sites, this could be what is observed in our case as well [36,38,39,44].

In Figs. 7 and 8, we observed a growing negative peak at 1335 and 1177 cm^{-1} under NO flow. The 1335 and 1177 cm^{-1} band pair was attributed to asymmetric and symmetric stretching vibrations of SO_2, respectively. The negative peaks indicate that these species were either displaced from the surface or transformed to other species after NO was introduced. Yang et al. also observed the same phenomenon on sulfated TiO_2 under NO flow [35]. This phenomenon seems to be enhanced in the presence of Gd–Pd as seen by the larger negative peak with NO exposure time.

After NO adsorption at room temperature, the sulfated surface (both TiO_2 and Gd–Pd/TiO_2) was flushed and heated in He to observe desorption of adspecies, as shown in Figs. 9 and 10. Over TiO_2, the HNO_2-like species at 1685 cm^{-1} was seen to desorb by 250 °C. This species seemed to be thermally transformed into other nitrogen-containing surface species. Concurrently, the bands at 1178 and 1619 cm^{-1}

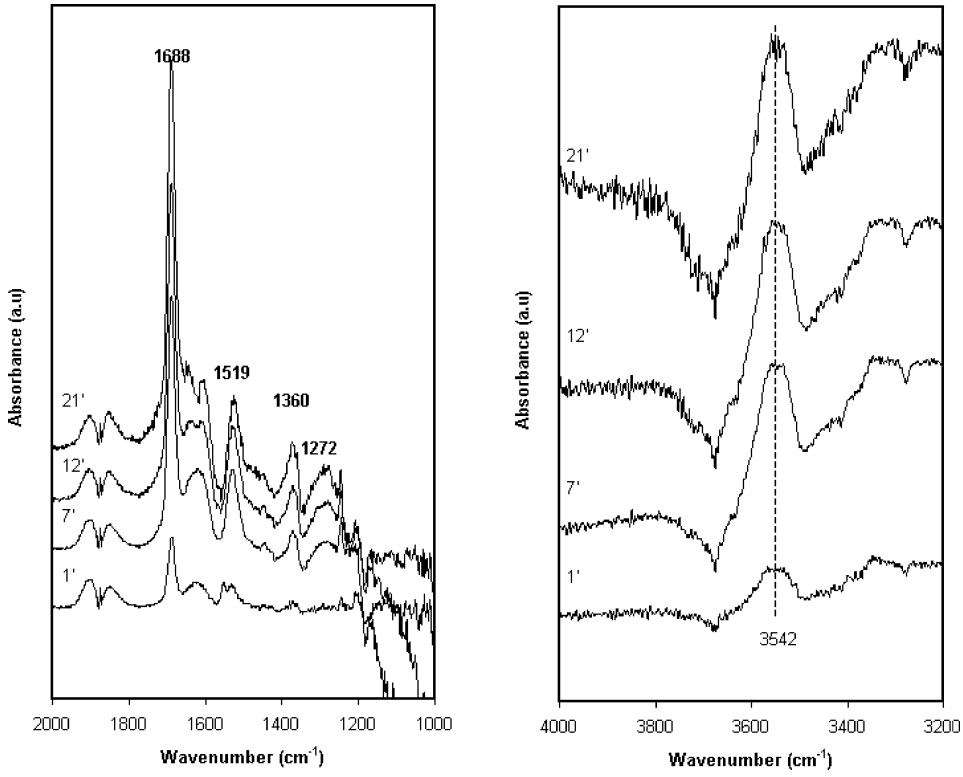

Fig. 7. DRIFT spectra of sulfated TiO_2 under 5000 ppm NO in He flow.

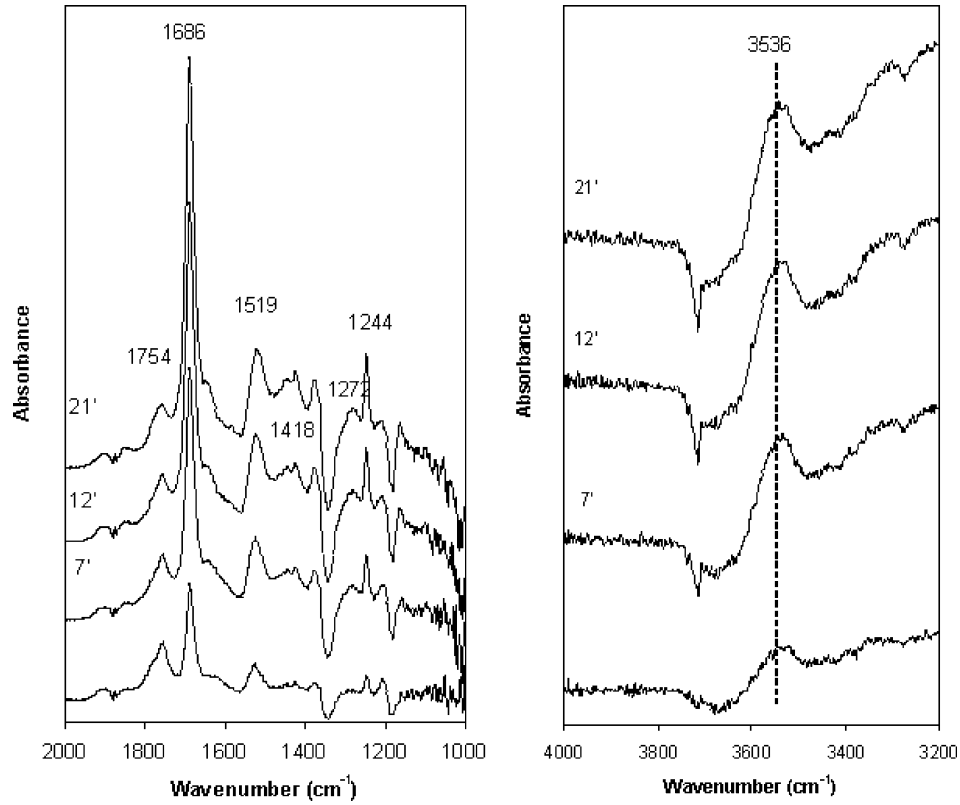

Fig. 8. DRIFT spectra of sulfated Gd–Pd/TiO_2 under 5000 ppm NO in He flow.

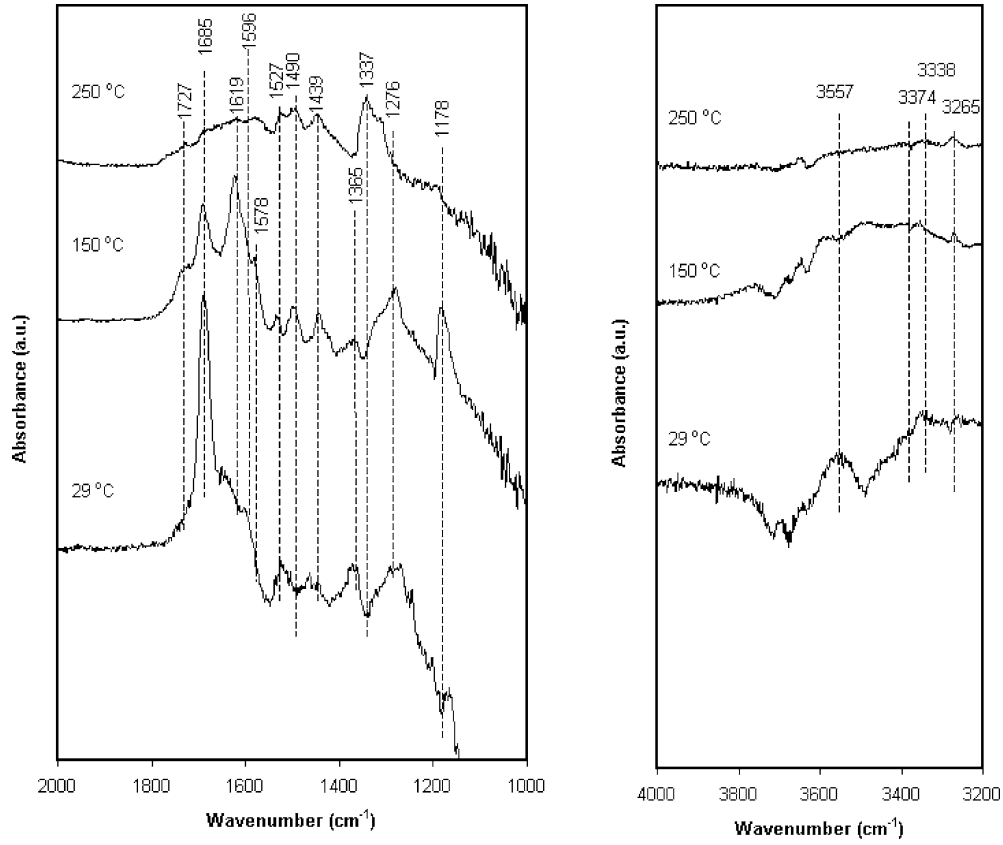

Fig. 9. TPD-DRIFT spectra of sulfated TiO_2 following NO exposure.

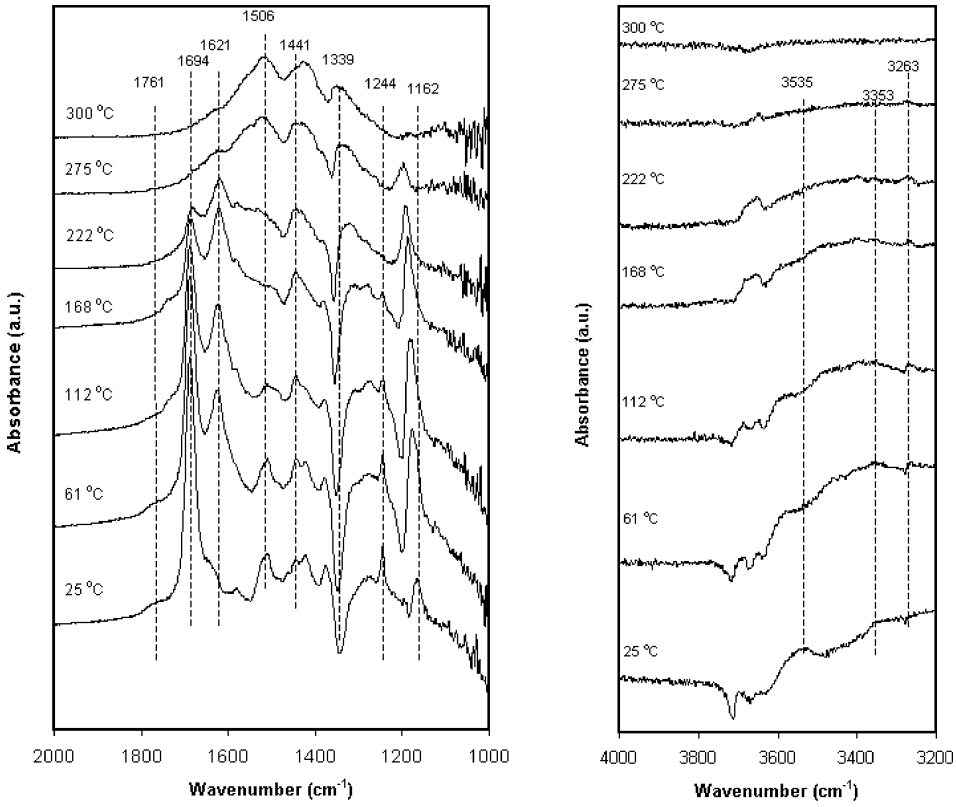

Fig. 10. TPD-DRIFT spectra of sulfated Gd–Pd/TiO_2 following NO exposure.

seem to grow. The band at 1619 cm^{-1} was assigned to bridge nitrate species [31–33]. The band at 1178 cm^{-1} was attributed to characteristic frequencies of NH_{3sy} coordinated to β (five-coordinated Ti^{4+}) Lewis acid site [44]. We also verified the formation of NH_x species by the characteristic IR peaks of 3265, 3338, and 3374 cm^{-1} for N–H stretching, which corresponds to molecularly adsorbed NH_3 on Lewis acid sites. It is interesting that even after SO_2 adsorption at 300 °C, there are still chemisorbed hydrogen atoms available on the surface to form NH_3. Similar observations were made on the nonsulfated Gd–Pd/TiO catalyst surface following NO adsorption. It is conceivable that chemisorbed hydrogen left on the surface from the reduction step reacts with adsorbed NO to form ammonia, which is coordinated on Lewis acid sites. The band positions for the surface NH_x species have been verified by adsorbing NH_3 on the same catalyst surfaces and observing the IR bands. The surface species at 250 °C on titania (monodentate nitrate, nitro species) are very similar to those observed on unsulfated titania surface after NO adsorption and heating, as shown in the previous study [26], indicating that SO_2 exposure does not seem to have an irreversible effect on the TiO_2 surface characteristics.

Fig. 10 shows the spectra taken under He with increasing surface temperature after NO was adsorbed on sulfated Gd–Pd/TiO_2 catalyst. The trend seen over both the support and the catalyst seems to be very similar. The 1685 cm^{-1} band decreased in intensity with temperature; however, concurrently, bridging nitrate species (1621 cm^{-1}) and NH_x species (1162 cm^{-1} for NH_{3sy}; 3263/3353 cm^{-1} for N–H) were formed. The negative peaks at 1339 and 1180 cm^{-1} seemed to grow in intensity up to 112 °C, but diminished above 168 °C. It is possible that sulfite species go through a chemical transformation, such as being converted to sulfate species in the presence of adsorbed NO. In fact, there were small bands around 1370 and 1430 cm^{-1} that were assigned previously to nitrospecies [26]; however, sulfate species are also known to exhibit bands in the same region, so the presence of sulfate species on the surface remains a distinct possibility [41–43,50]. It is also conceivable that these chemical transformations are reversed above 168 °C, as bridged nitrate and NH_x species are desorbed. This results in the reappearance of sulfite-like species due to desorption of N-containing adspecies.

The band that corresponds to Pd^0–NO species ($\sim$1745 cm^{-1}) on reduced Gd–Pd/TiO_2 after NO adsorption was previously found to shift toward higher wavenumbers with increasing intensity as a function of temperature [26,48]. It was also the predominant NO adspecies observed at higher temperatures on the catalyst, possibly forming by decomposition/transformation of nitrate-type species and appearing at the 1780–1790 cm^{-1} range [26]. Interestingly, over the SO_2-exposed catalyst, the weak band that was observed at 1761 cm^{-1} at room temperature disappeared at higher temperatures and a band at $\sim$1790 cm^{-1} never appeared. Lack of Pd–NO formation on a sulfated catalyst

seems to suggest that either Pd sites are unable to readsorb NO (blockage of Pd) or availability of NO_x adspecies is limited (inhibition of NO transfer) on the sulfated catalyst. The latter supposition could be supported by the NO TPD results, which indicated that the overall capacity to reversibly adsorb NO was severely retarded due to sulfation. It is conceivable that the inability of the catalyst to form Pd–NO on the sulfated surface may account for the poor NO reduction activity because linearly adsorbed NO species are believed to be one of the key surface intermediates which react with CH_x and NH_x species to form N_2.

4. Conclusions

In situ DRIFTS and TPD were used to investigate the effect of SO_2 on the nature of NO adsorption sites for Pd and Gd–Pd catalysts supported on TiO_2. The steady-state reaction results in the presence of SO_2 showed that the Gd-containing catalysts have a higher resistance to SO_2 deactivation compared to the Gd-free catalysts [24]. In situ DRIFT spectra revealed that the presence of SO_2 in the feed affected the bond strength of Pd and NO by possibly altering the electron density at the Pd sites. The presence of Gd, through its electropositive nature, seemed to minimize this effect by providing electrons to Pd atoms. TPD results showed that SO_2 inhibited the formation of Pd–NO species as evidenced by the disappearance of the high temperature feature. The IR data also supported this supposition since Pd–NO species (1790 cm^{-1} band) were not observed after the catalyst was exposed to high SO_2 concentration.

In summary, we can conclude that the catalyst deactivation in the presence of SO_2 was caused by the inhibition of Pd–NO species, which are believed to be one of the key surface intermediates in the reduction scheme. The fact that Gd incorporation partially prevents or slows down the deactivation process suggests that the effect of SO_2 is not a simple site blockage phenomenon, but is related to changes in the electron density at Pd sites. Studies are underway to examine the reversibility of the deactivation process.

Acknowledgments

The financial contributions from the National Science Foundation and the Ohio Coal Development Office are gratefully acknowledged.

References

[1] Y. Li, J.N. Armor, Appl. Catal. B 1 (4) (1992) L31.
[2] Y. Li, J.N. Armor, Appl. Catal. B 3 (1993) L1.
[3] Y. Li, J.N. Armor, J. Catal. 145 (1994) 1.
[4] Y. Li, J.N. Armor, J. Catal. 150 (1994) 376.
[5] Y. Nishizaka, M. Misono, Chem. Lett. (1993) 1295.
[6] K. Yogo, M. Umeno, H. Watanabe, E. Kikuchi, Catal. Lett. 19 (1993) 131.
[7] R. Burch, S. Scire, Appl. Catal. B 3 (1994) 295.
[8] B.J. Adelman, W.M.H. Sachtler, Appl. Catal. B 14 (1997) 1.
[9] L.J. Lobree, A.W. Aylor, J.A. Reimer, A.T. Bell, J. Catal. 169 (1997) 188.
[10] A.D. Cowan, N.W. Cant, B.S. Haynes, P.F. Nelson, J. Catal. 176 (1998) 329.
[11] J.-Y. Yan, H.H. Kung, W.M.H. Sachtler, M.C. Kung, J. Catal. 175 (1998) 294.
[12] X. Zhang, A.B. Walters, M.A. Vannice, J. Catal. 155 (1995) 290.
[13] S.-J. Huang, A.B. Walters, M.A. Vannice, J. Catal. 192 (2000) 29.
[14] M.D. Fokema, J.Y. Ying, Appl. Catal. B 18 (1998) 71.
[15] M.W. Kumthekar, U.S. Ozkan, J. Catal. 171 (1997) 45.
[16] M.W. Kumthekar, U.S. Ozkan, J. Catal. 171 (1997) 54.
[17] M.W. Kumthekar, U.S. Ozkan, J. Catal. 171 (1997) 67.
[18] U.S. Ozkan, M.W. Kumthekar, G. Karakas, Catal. Today 40 (1998) 3.
[19] Y. Li, J.N. Armor, Appl. Catal. B 5 (1995) L257.
[20] G. Zhang, T. Yamaguchi, H. Kawakami, T. Suzuki, Appl. Catal. B 1 (3) (1992) L15.
[21] W. Li, M. Sirilumpen, R.T. Yang, Appl. Catal. B 11 (1997) 347.
[22] H.S. Gandhi, M. Shelef, Appl. Catal. 77 (1991) 175.
[23] J. Mitome, G. Karakas, K.A. Bryan, U.S. Ozkan, Catal. Today 42 (1998) 3.
[24] J. Mitome, E. Aceves, U.S. Ozkan, Catal. Today 53 (1999) 597.
[25] J.M. Watson, U.S. Ozkan, J. Mol. Catal. A 3979 (2002) 1.
[26] J.M. Watson, U.S. Ozkan, J. Catal. 210 (2002) 295.
[27] T.E. Hoost, K. Otto, K.A. Laframboise, J. Catal. 155 (1995) 303.
[28] T. Solomun, J. Electroanal. Chem. 199 (1986) 443.
[29] S. Moriki, Y. Inoue, E. Miyazaki, I. Yasumori, J. Chem. Soc., Faraday Trans. 78 (1982) 171.
[30] C.M. Grill, R.D. Gonzalez, J. Phys. Chem. 84 (1980) 878.
[31] S.-J. Huang, A.B. Walters, M.A. Vannice, Appl. Catal. B 26 (2000) 101.
[32] A.A. Davydov, Infrared Spectroscopy of Adsorbed Species on the Surface of Transition Metal Oxides, Wiley, Chichester, 1990.
[33] Y. Chi, S.C. Chuang, J. Phys. Chem. B 104 (2000) 4673.
[34] G. Ramis, G. Busca, V. Lorenzelli, P. Forzatti, Appl. Catal. 64 (1990) 243.
[35] R.T. Yang, W.B. Li, N. Chen, Appl. Catal. A 169 (1998) 215.
[36] M. Ziolek, I. Sobczak, I. Nowak, M. Daturi, J.C. Lavalley, Top. Catal. 11/12 (2000) 343.
[37] G. Larsen, E. Lotero, R.D. Parra, L.M. Petkovic, H.S. Silva, S. Raghavan, Appl. Catal. A 130 (1995) 213.
[38] Y.-H. Chin, A. Pisanu, L. Serventi, W.E. Alvarez, D.E. Resasco, Catal. Today 54 (1999) 419.
[39] S.M. Jung, P. Grange, Appl. Catal. B 27 (2000) L11.
[40] J. Wang, C. Li, Appl. Surf. Sci. 161 (2000) 406.
[41] D. Lin-Vien, N.B. Colthup, W.G. Fateley, J.G. Grasselli, The Handbook of Infrared and Raman Characteristic Frequencies of Organic Molecules, Academic Press, San Diego, CA, 1991.
[42] J.P. Chen, R.T. Yang, J. Catal. 139 (1993) 277.
[43] O. Saur, M. Bensitel, A.B.M. Saad, J.C. Lavalley, C.P. Tripp, B.A. Morrow, J. Catal. 99 (1986) 104.
[44] K. Hadjiivanov, V. Bushev, M. Kantcheva, D. Klissurski, Langmuir 10 (1994) 464.
[45] A. Datta, R.G. Cavell, J. Phys. Chem. 89 (1985) 443.
[46] A. Rath, E. Aceves, J. Mitome, J. Liu, U.S. Ozkan, S.G. Shore, J. Mol. Catal. A 165 (2001) 103.
[47] C. Yanxin, J. Yi, L. Wenzhao, J. Rongchao, T. Shaozhen, H. Wenbin, Catal. Today 50 (1999) 39.
[48] K. Almusaiteer, S.S.C. Chuang, J. Catal. 184 (1999) 189.
[49] K. Nakamoto, Infrared Spectra of Inorganic and Coordination Compounds, Wiley, New York, 1970.
[50] M. Zillek, I. Sobczak, I. Nowak, M. Daturi, J.C. Lavalley, Top. Catal. 11/12 (2000) 343.